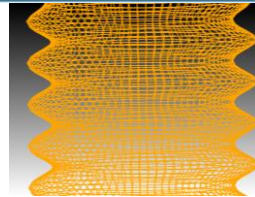
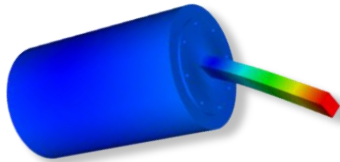
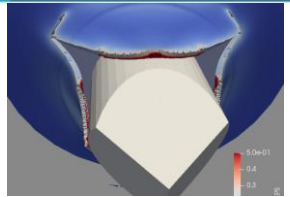
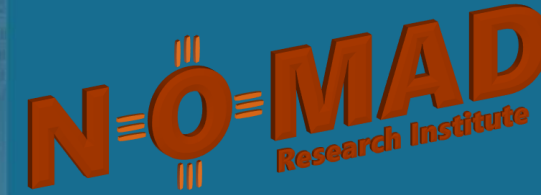




Sandia National Laboratories

Ductile Failure Prediction in Additively Manufactured Metals via 3D Characterization



Thomas Cisneros
Ivana Hernandez
Suhanna Bamzai

Mentors: Andrew Polonsky (lead), Ashley Spear, John Emery, Chad Hovey, Dan Moser, Paul Chao



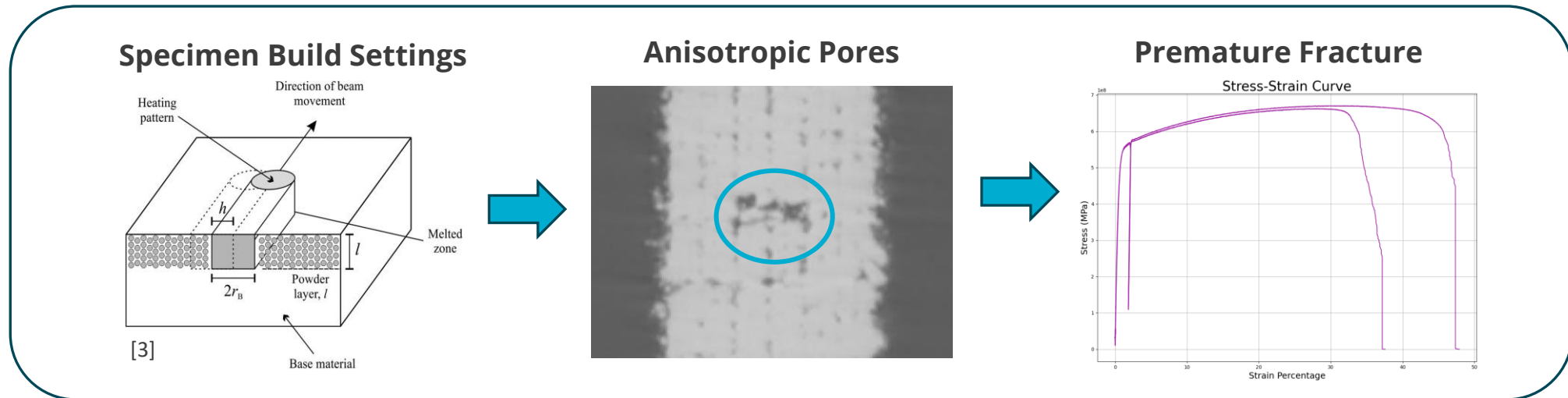
Sandia National Laboratories is a multimission laboratory managed and operated by National Technology & Engineering Solutions of Sandia, LLC, a wholly owned subsidiary of Honeywell International Inc., for the U.S. Department of Energy's National Nuclear Security Administration under contract DE-NA0003525.

SAND2024-10177PE

Motivation



- Increasing need for reliability and safety (Ex: Automotive, Healthcare, Aerospace)
- **Additive Manufacturing (AM):**
 - Produces complex geometries with unprecedented design freedom and customization
 - Generates non-uniform material properties, extreme anisotropy, and ***inherent porosity*** [1, 2].

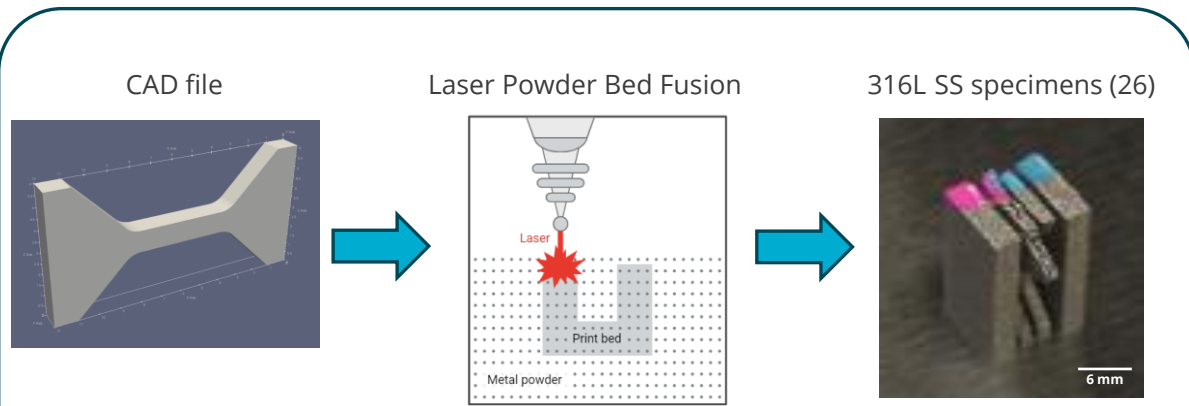


Goal: Validate different failure prediction approaches given the set of experimental data.

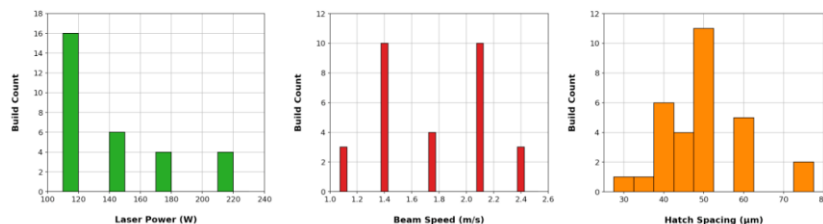
- **Prediction models:**
 - Direct Numerical Simulation (DNS): Gold standard of failure prediction [3, 4].
 - Void Descriptor Function (VDF): Lightweight prediction model [5-6].



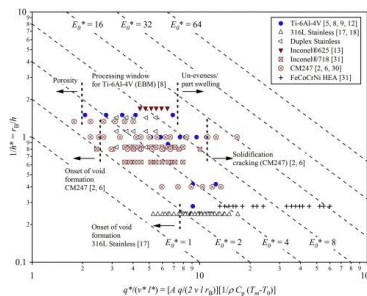
Additive Manufacturing of Samples



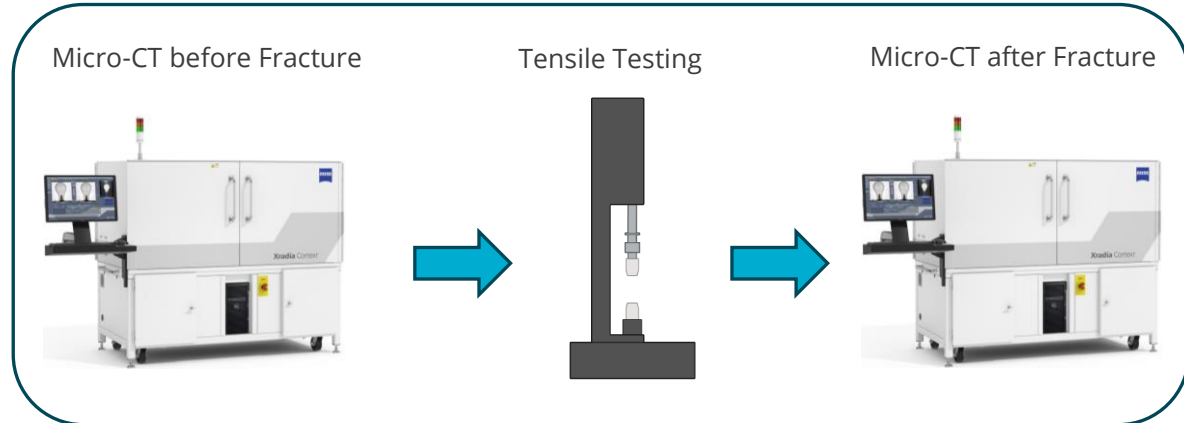
Fabrication Parameters



Normalized Energy Calculations [7]



3D Characterization Techniques



Data Acquisition

As-Built Samples

Grayscale Segmented

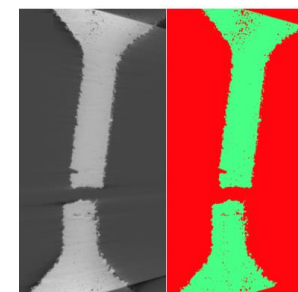


Stress-Strain Data

| Stress (MPa) | Strain (%) |
|--------------|------------|
| 26.8918 | -0.00402 |
| 27.11515 | 0.001831 |
| 27.47726 | 0.00209 |
| 27.78574 | 0.001993 |
| 28.35874 | 0.001997 |

Fractured Samples

Grayscale Segmented





Raw and Segmented Data

As-Built Samples

Grayscale Segmented

Stress-Strain Data

| Stress (MPa) | Strain (%) |
|--------------|------------|
| 26.8918 | -0.00402 |
| 27.11515 | 0.001831 |
| 27.47726 | 0.00209 |
| 27.78574 | 0.001993 |
| 28.35874 | 0.001997 |

Fractured Samples

Grayscale Segmented

Image and data Pre-processing

Stress-Strain normalization

↓

Crop Data

↓

recon3d
GitLab Repository

Binary to Semantic

↓

Instance Analysis
Pore Processing

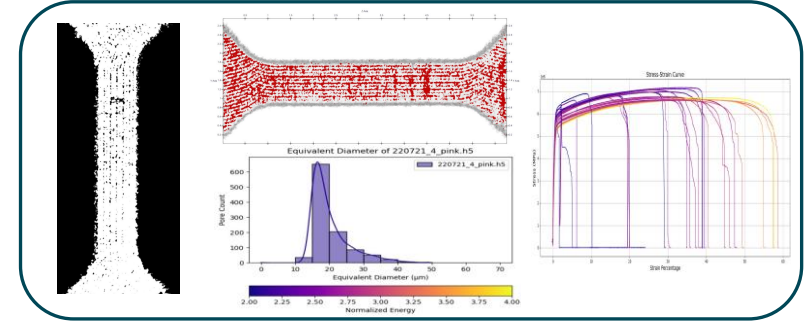
↓

Downscale

↓

npz to Mesh

Experimental Data Analysis



Direct Numerical Simulations (DNS)

Sierra/SM

```

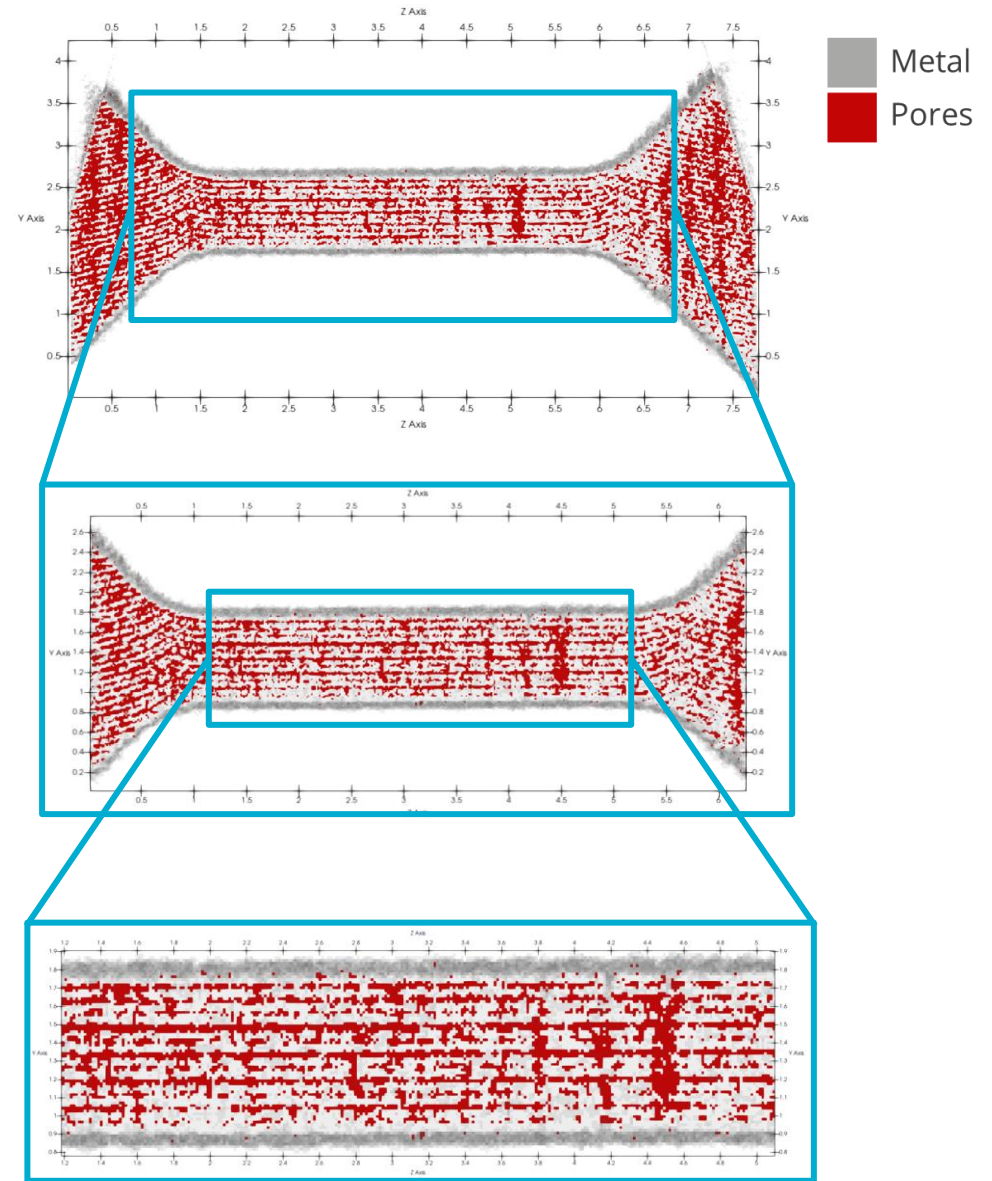
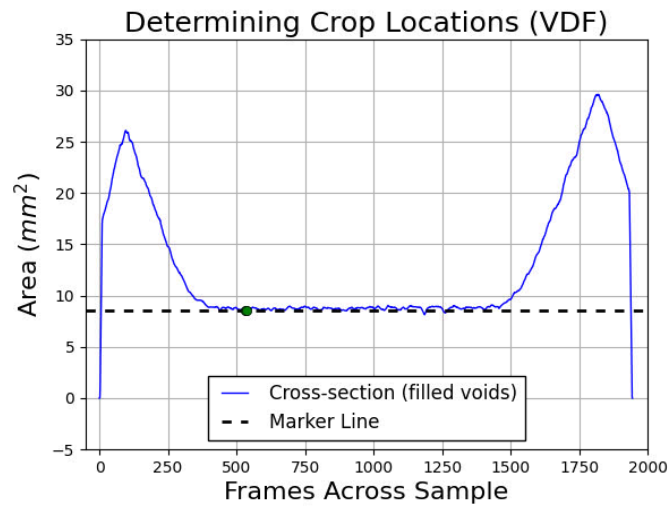
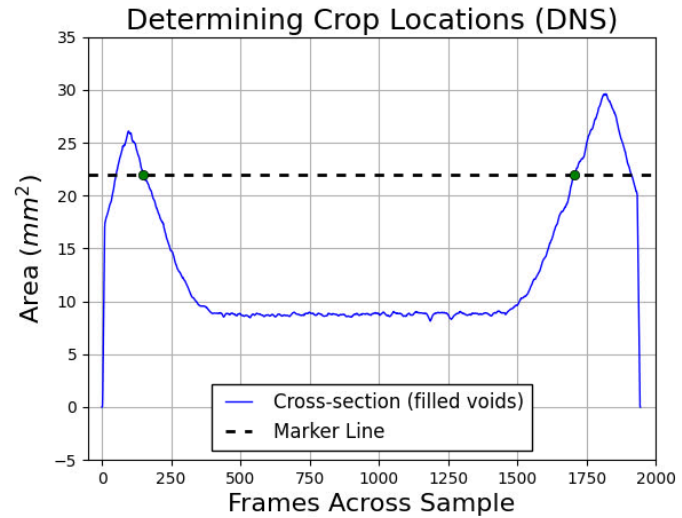
24 # Table of Contents
25 # > Begin Sierra
26 # > Input Parameters
27 # > Points/Directions/Axes/Coordinate Systems
28 # > Functions
29 # > Materials
30 # > Finite Element Model
31 # > Sections
32 # > Rigid Bodies
33 # > Procedure
34 # > Time Control
35 # > Region
36 # > Initial Conditions
37 # > Boundary Conditions
38 # > Constraints
39 # > Contact
40 # > Element Death
41 # > Output
42 # > Solver
    
```

Void Descriptor Function (VDF)

- pores
- axis_vectors
- centroids
- ellipsoid_surface_areas
- ellipsoid_volumes
- equivalent_sphere_diameters
- nearest_neighbor_IDs
- nearest_neighbor_distances
- num_voxels
- semi-axis_lengths

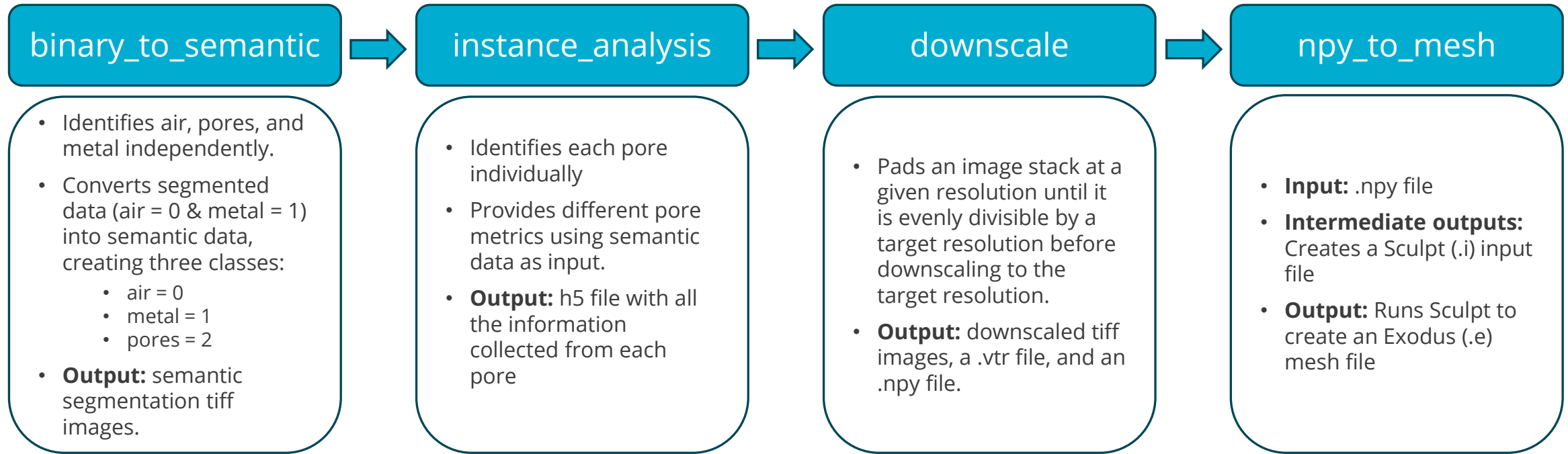
220719_5_blue.csv

Methods: Pre-processing (Crop Data)



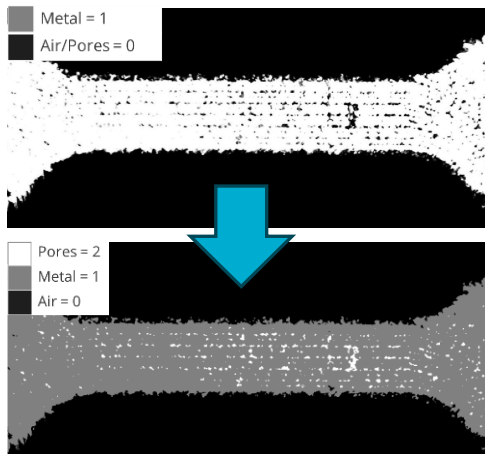
recon3d

GitLab Repository



binary_to_semantic

- Identifies air, pores, and metal independently.
- Converts segmented data (air = 0 & metal = 1) into semantic data, creating three classes:
 - air = 0
 - metal = 1
 - pores = 2
- **Output:** semantic segmentation tiff images.



instance_analysis

- Identifies each pore individually
- Provides different pore metrics using semantic data as input.
- **Output:** h5 file with all the information collected from each pore

- pores
 - axis_vectors
 - centroids
 - ellipsoid_surface_areas
 - ellipsoid_volumes
 - equivalent_sphere_diameters
 - nearest_neighbor_IDs
 - nearest_neighbor_distances
 - num_voxels
 - semi-axis_lengths

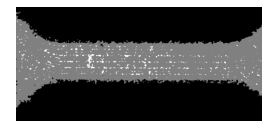
downscale

- Pads an image stack at a given resolution until it is evenly divisible by a target resolution before downscaling to the target resolution.
- **Output:** downsampled tiff images, a .vtr file, and an .npy file.

Resolution = 4 μm

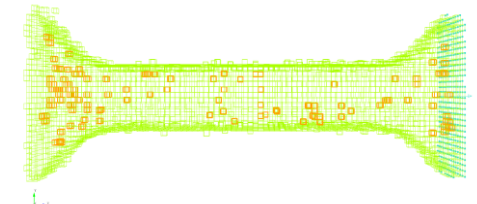


Resolution = 20 μm

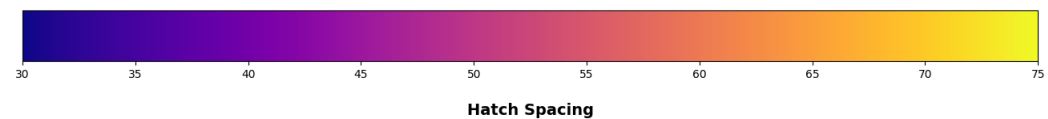
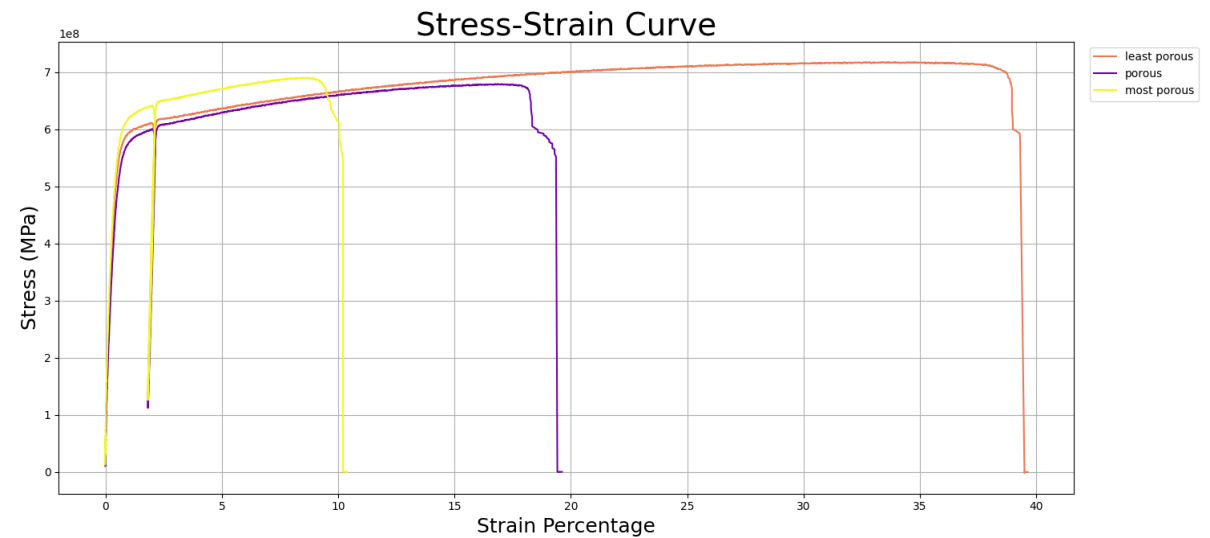
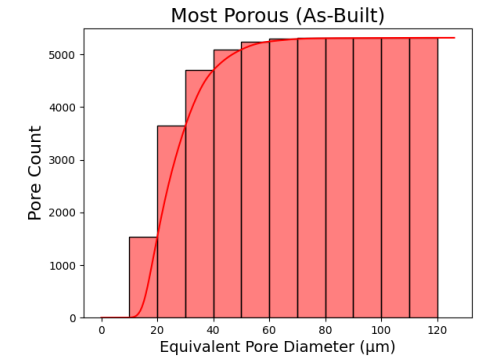
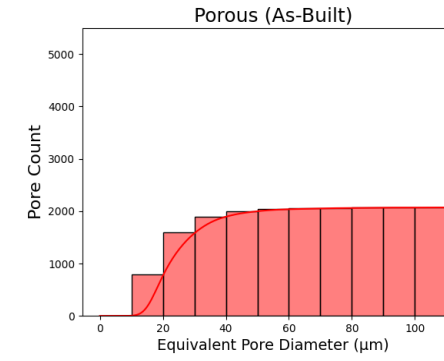
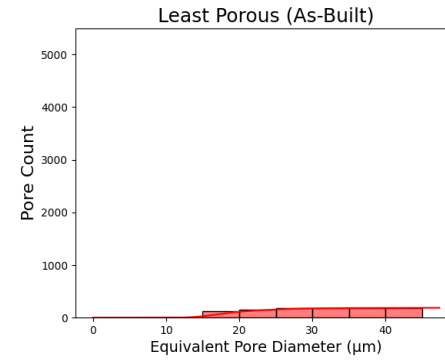
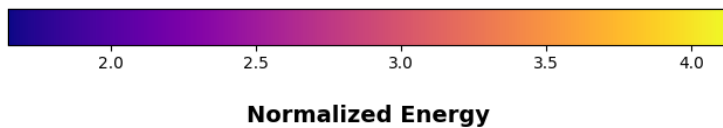
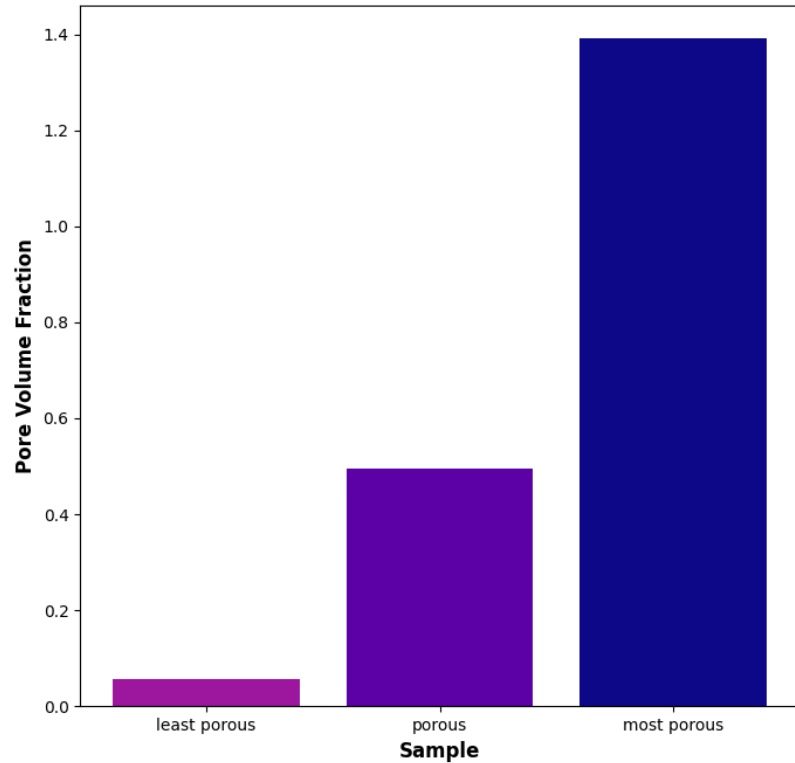


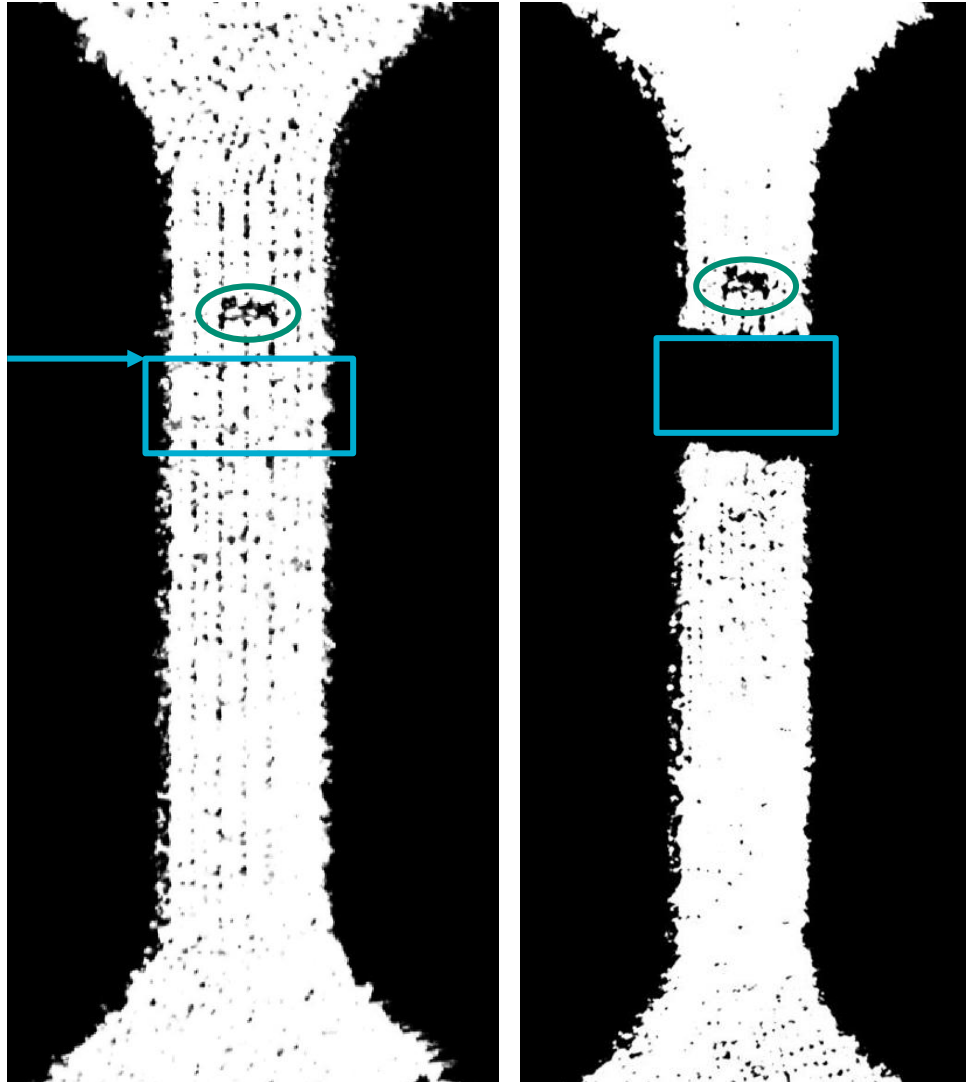
npy_to_mesh

- **Input:** .npy file
- **Intermediate outputs:** Creates a Sculpt (.i) input file
- **Output:** Runs Sculpt to create an Exodus (.e) mesh file



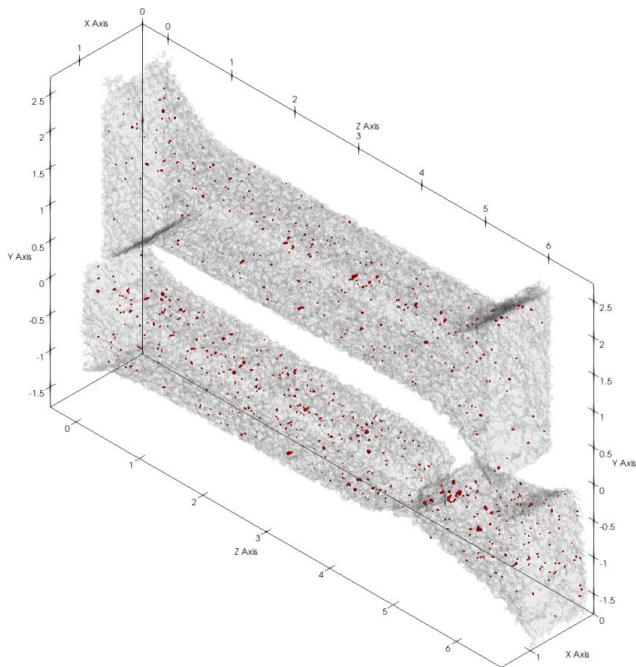
Methods: Pre-Processing (Pore Statistics)



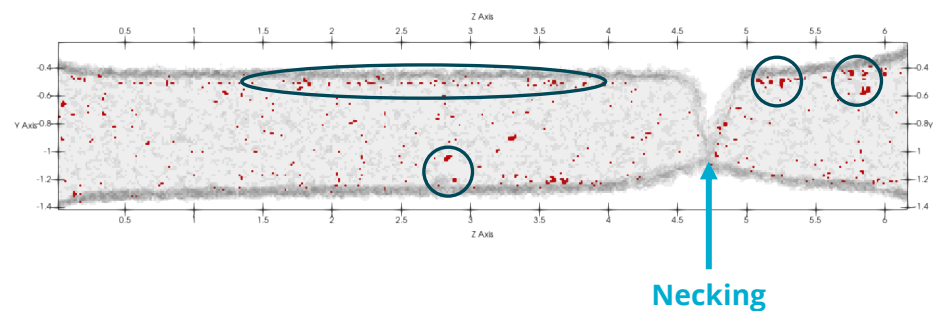
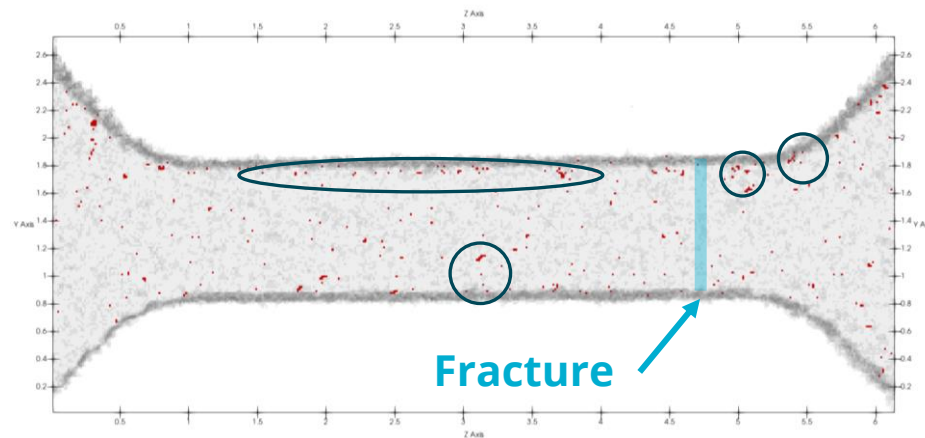
As-Built**Fractured**

- Image J was used to manually locate fracture site.
- Pixel (2D) data was given which was converted to real space data in μm .
- ParaView was utilized to visualize both the as-built and fractured samples to identify the fracture location.
- This method was applied for all 26 samples.

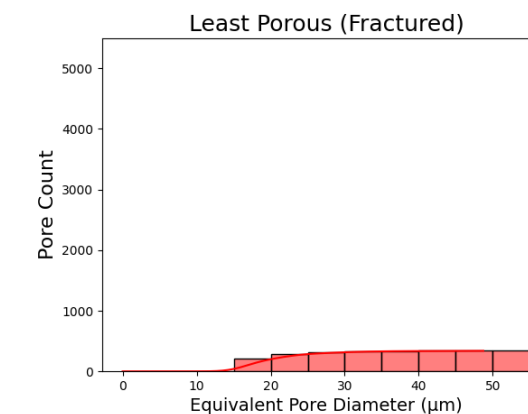
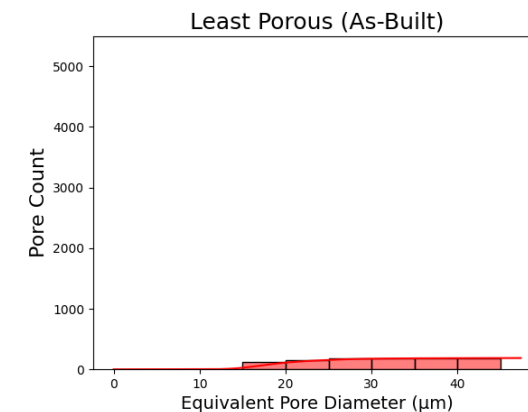
Least Porous



Scale is in mm



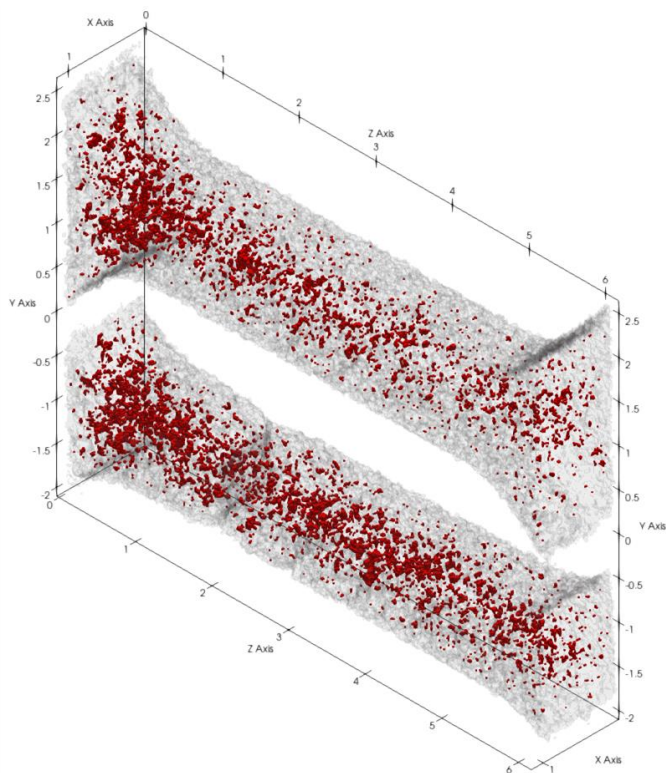
Fracture Location \approx 4.692 mm



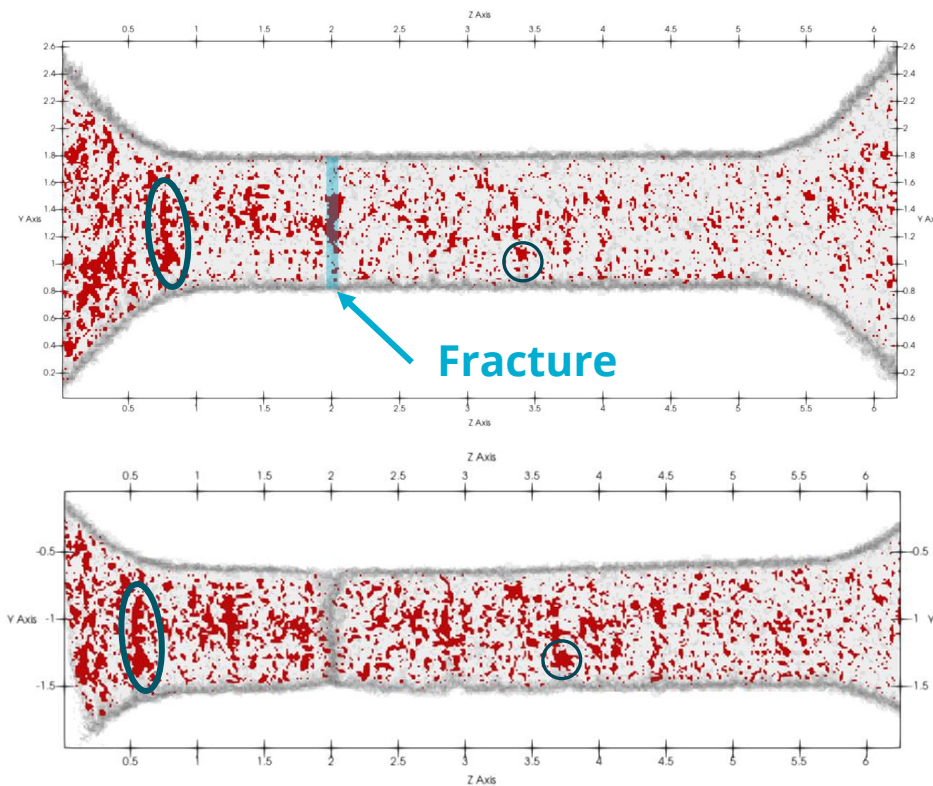
Equivalent diameter 0.22% increase



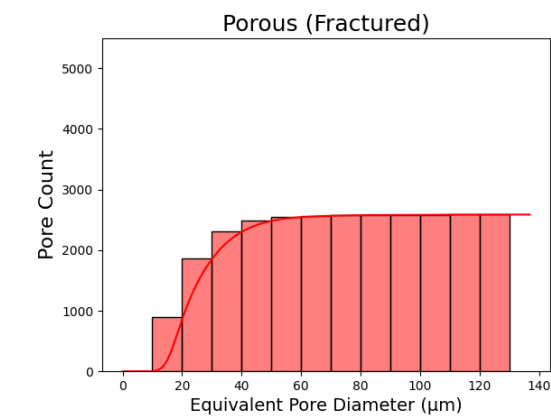
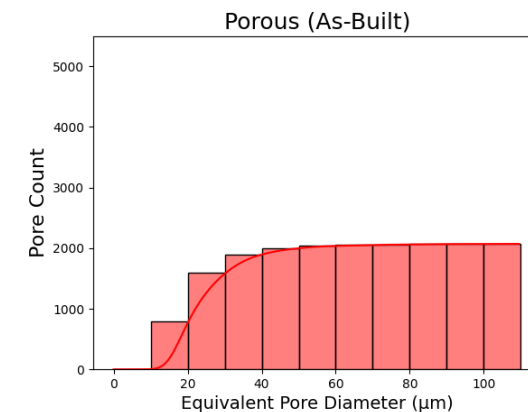
Porous



Scale is in mm



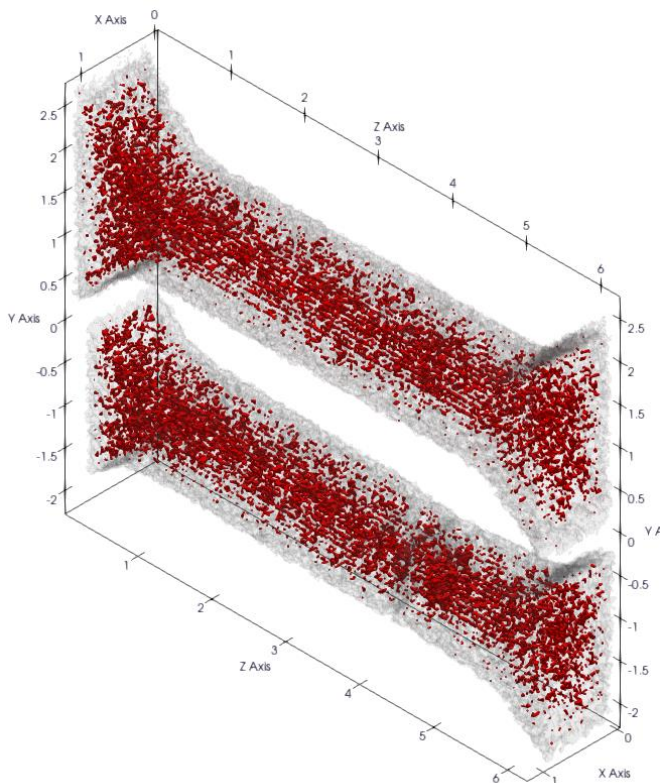
Fracture Location ≈ 2.048 mm



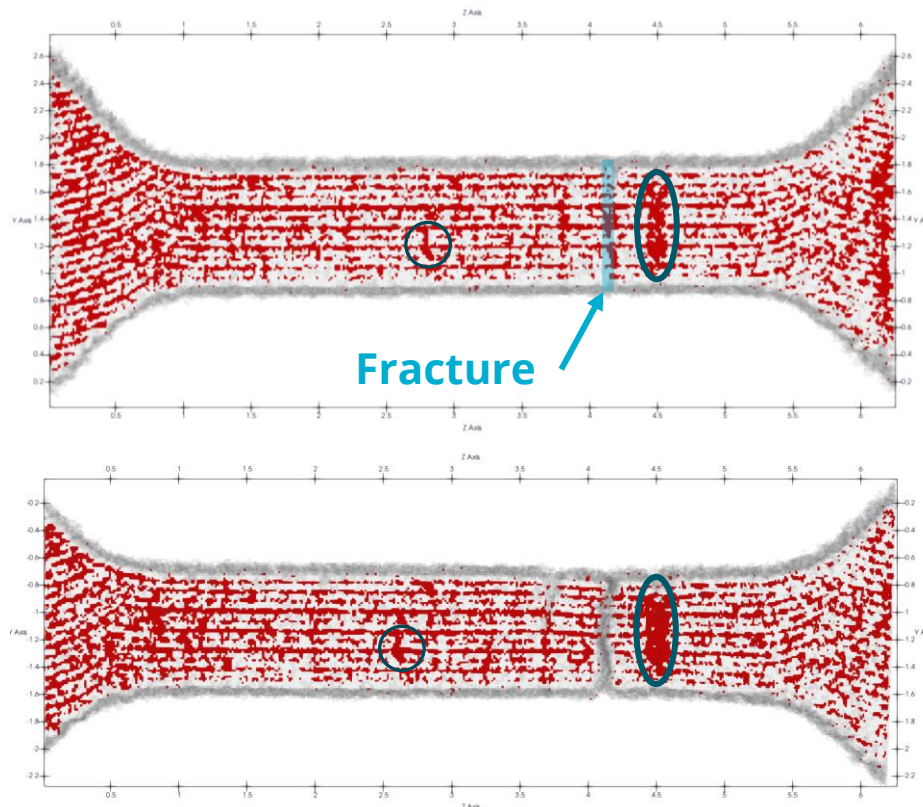
Equivalent diameter 4.36% increase



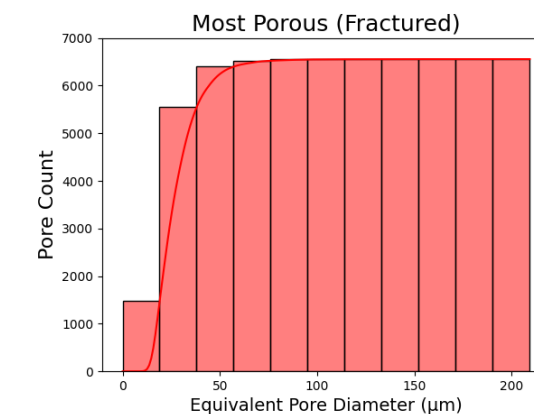
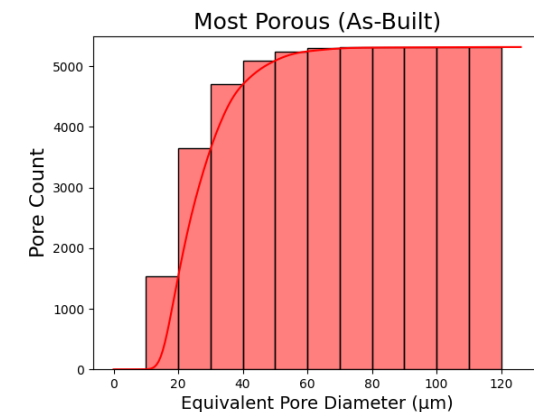
Most Porous



Scale is in mm

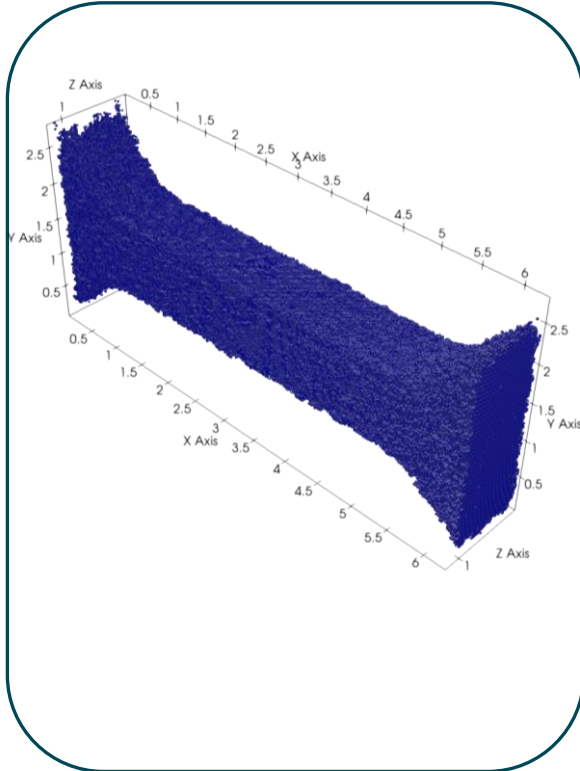


Fracture Location ≈ 4.184 mm



Equivalent diameter 2.29% increase

Mesh creation –
voxel size



Sierra/SM simulation
workflow

- Select material model
- Material properties
- Build input deck
- Debug input deck

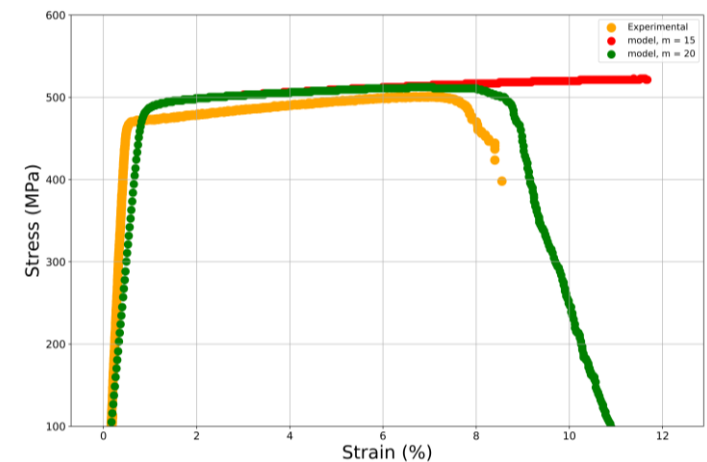
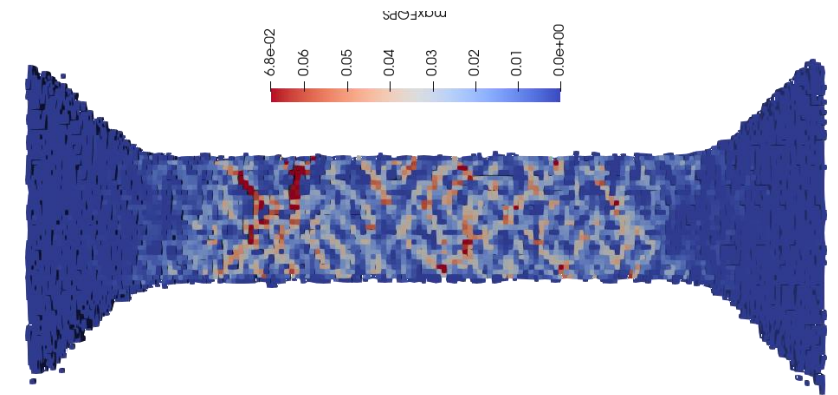


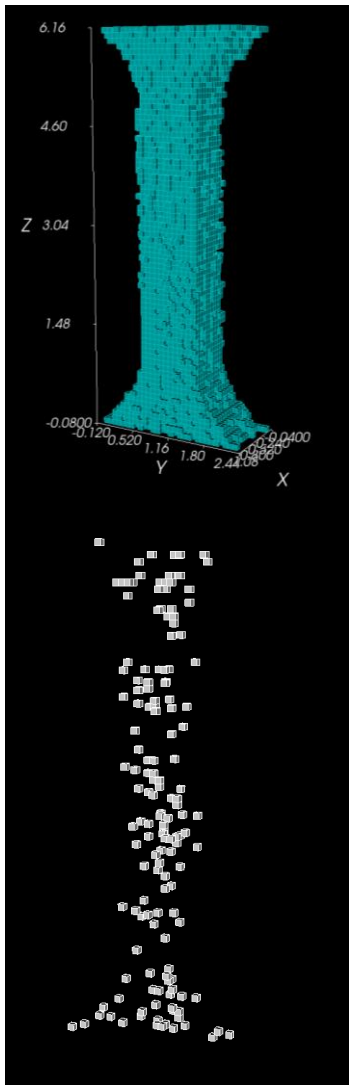
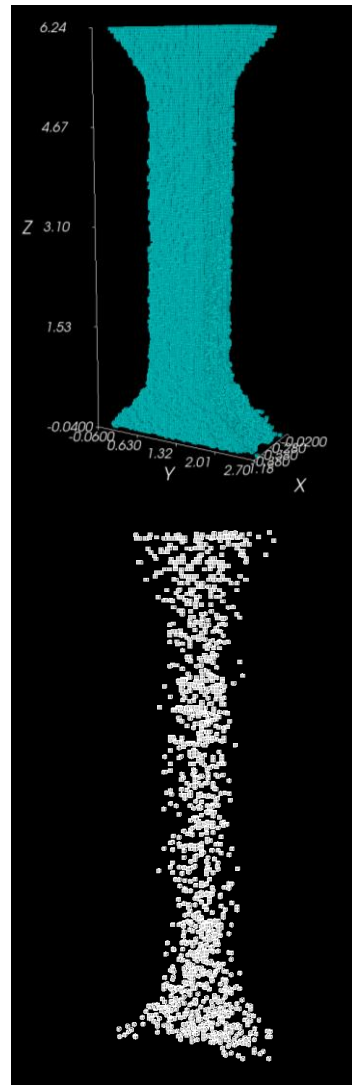
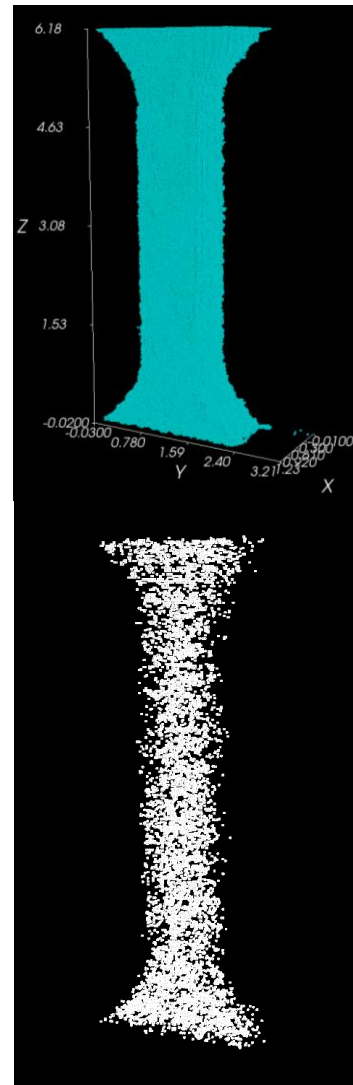
- Run simulations
- Calibrate parameters porous mesh



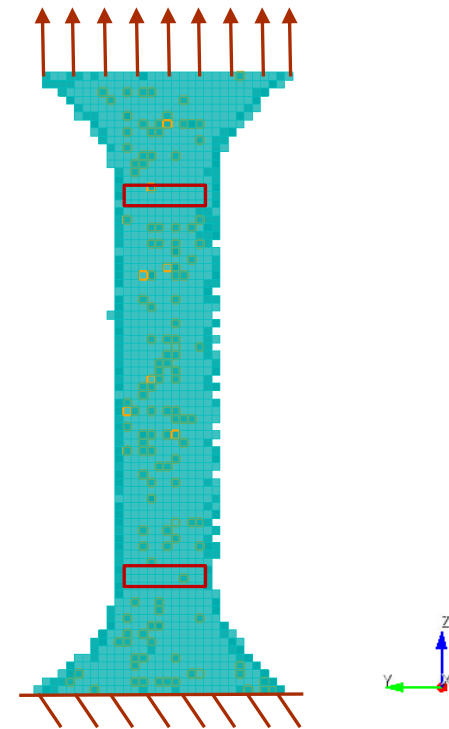
- Predict failure in porous samples
- Varying resolution simulations

Different sample
simulations



80 μm voxel40 μm voxel20 μm voxel

- CUBIT was utilized to add node sets to be used for boundary conditions.
- Pore elements deleted.



Methods: AM 316L SS property specification



- Hill plasticity model:
 - Anisotropic/rate dependent yield
 - Plasticity captured via Voce hardening
 - Scalar damage model

Hill plasticity

$$\theta^2(\hat{\sigma}_{ij}) = F(\hat{\sigma}_{22} - \hat{\sigma}_{33})^2 + G(\hat{\sigma}_{33} - \hat{\sigma}_{11})^2 + H(\hat{\sigma}_{11} - \hat{\sigma}_{22})^2 + 2L\hat{\sigma}_{23}^2 + 2M\hat{\sigma}_{31}^2 + 2N\hat{\sigma}_{12}^2$$

| Material Property | Variable | Value | Units |
|---------------------------------|-------------------------------------|---------|----------|
| Young's Modulus | E | 200e9 | Pa |
| Poisson's Ratio | v | 0.27 | - |
| Density | ρ | 7920 | Kg/m^3 |
| Material Parameter | Variable | Value | Units |
| Rate independent yield constant | Y_0 | 453.3e6 | Pa |
| Hill transverse yield ratio | $R_{11} = R_{33}$ | 1.124 | - |
| Remaining Hill yield ratios | $R_{22} = R_{12} = R_{13} = R_{23}$ | 1.0 | - |
| Voce hardening coef | A | 883.6e6 | Pa |
| Voce hardening exponential coef | b | 1.39 | - |
| Yield rate coef | f | 21012 | 1/s |
| Yield rate exponent | n | 10.06 | - |

Damaged Cauchy stress

$$\hat{\sigma}_{ij} = \sigma_{ij} / (1 - \phi)$$

↓
Void volume fraction

Voce Hardening

$$\sigma_f = Y_0 \left\{ 1 + \sinh^{-1} \left[\left(\frac{\dot{\epsilon}_p}{f} \right)^{1/n} \right] \right\} + A \left((1 - \exp(b\epsilon_p)) \right)$$

Yield ↓ Fitting constant ↓ Fitting exp

Results: Stress-strain response – different damage exponent (m)

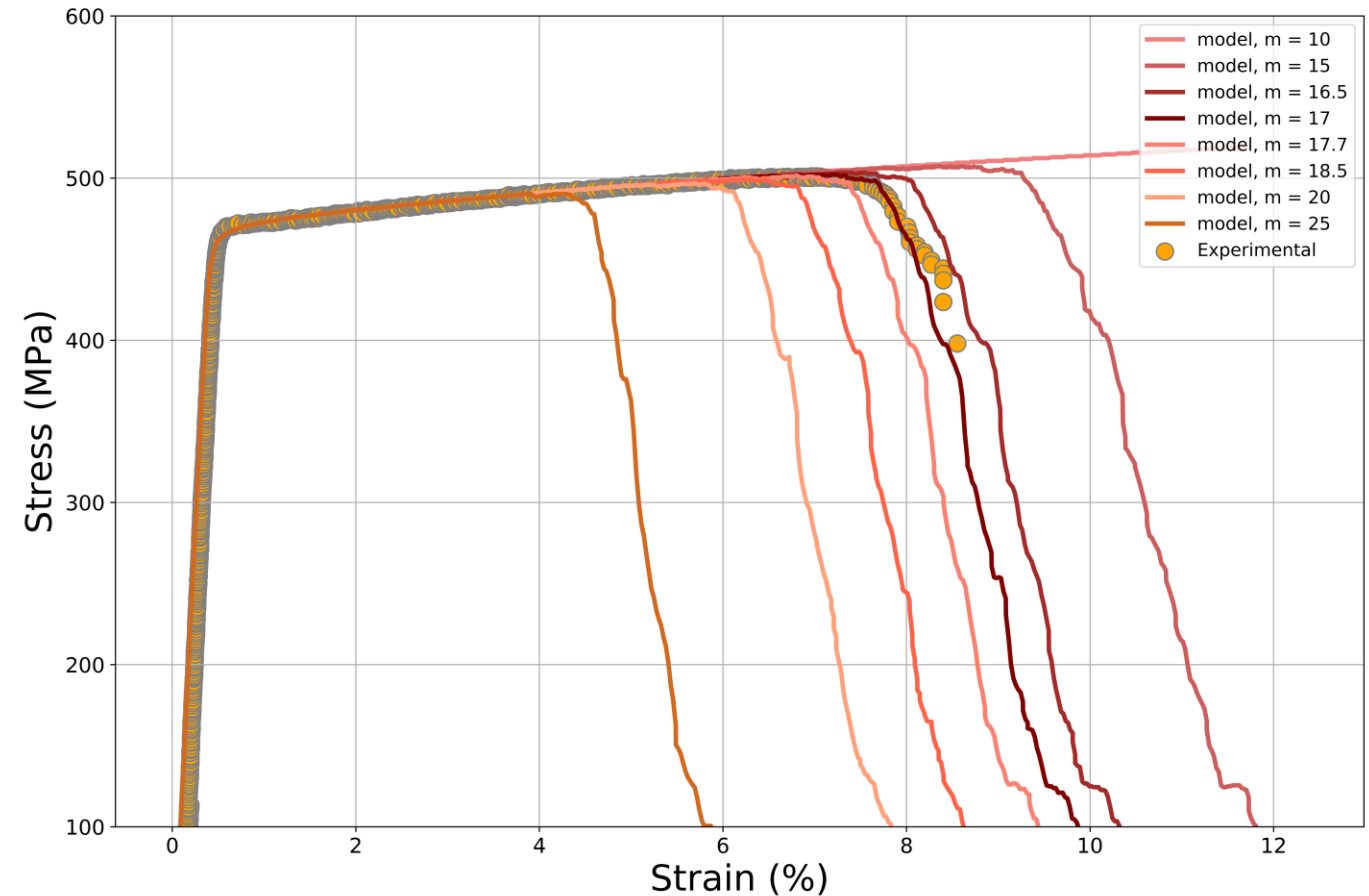


$m \propto \text{damage}$

$$\dot{v}_v = \sqrt{\frac{2}{3}} \dot{\epsilon}_p \frac{1}{\eta} (1 + \eta v_v) [(1 + \eta v_v)^{m+1} - 1]$$

$$\cdot \sinh \left[\frac{2(2m-1) \langle p \rangle}{2m+1 \sigma_f} \right] - (v_v - v_0) \frac{\dot{\eta}}{\eta}$$

40 μm voxel size

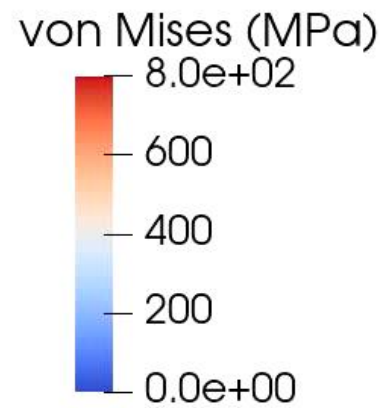
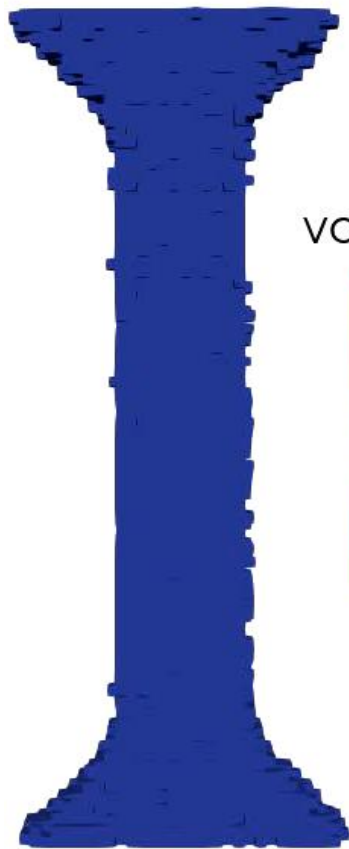


Results: Mesh size effect



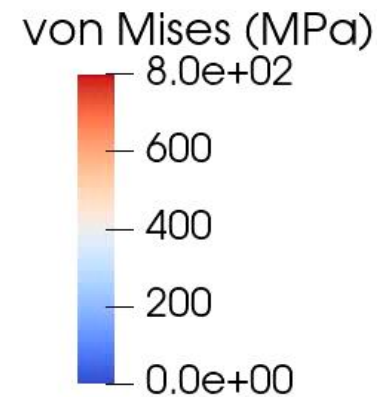
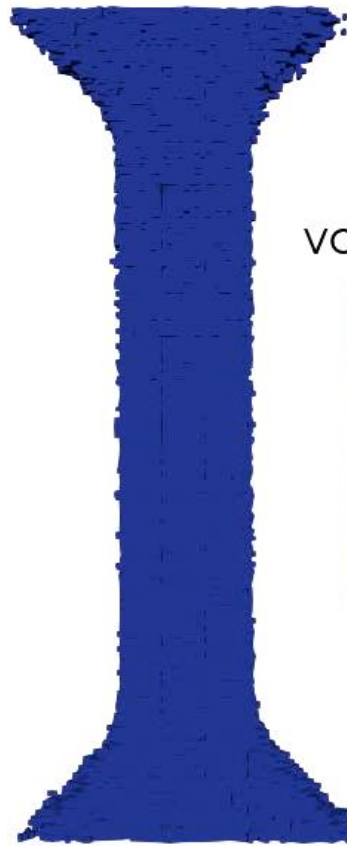
Porous

80 μm voxel



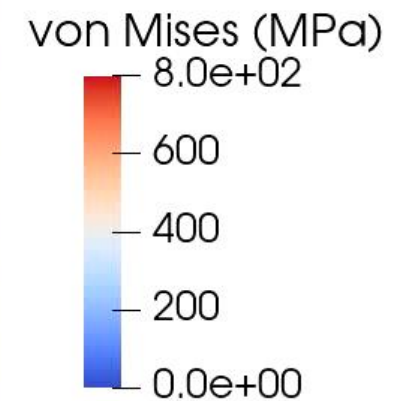
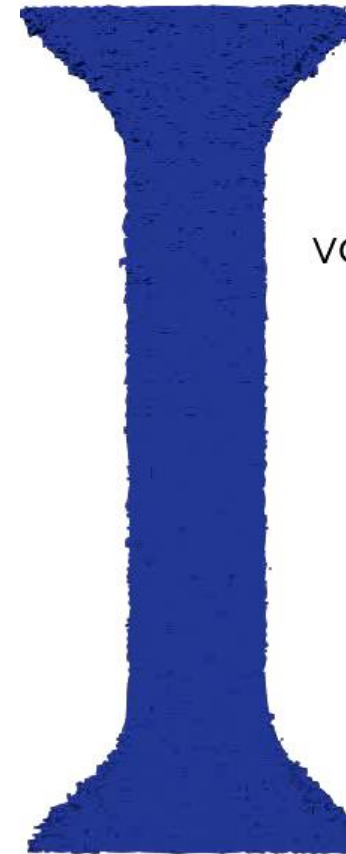
~13k elements
20 processors
0.25 hr wall time

40 μm voxel



~100k elements
40 processors
1.4 hr wall time

20 μm voxel



~800k elements
330 processors
2.46 hr wall time

Methods: Void Descriptor Function (VDF)

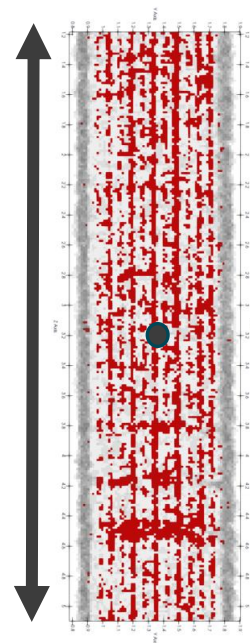
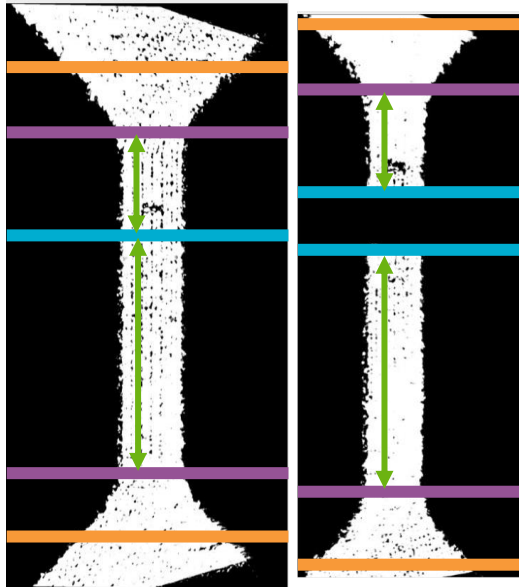


- Identifies positions along gauge section highly populated by critical pore structures [4]
 - Signals where fracture is likely to occur
- Quantifies the inter-relationships of pores to quickly predict failure [4]
 - Factors: pore location, size, and distance to free surface

Crop Data

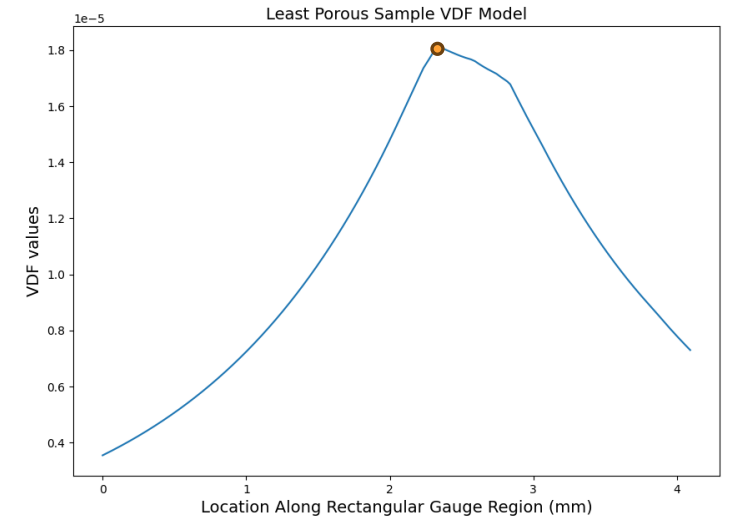
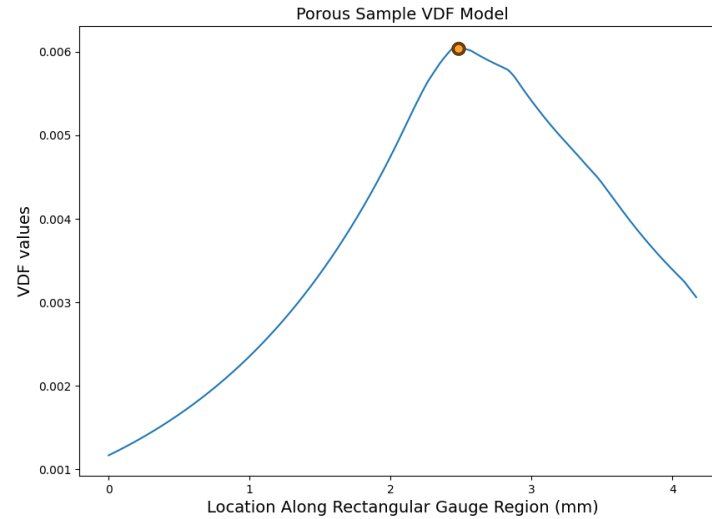
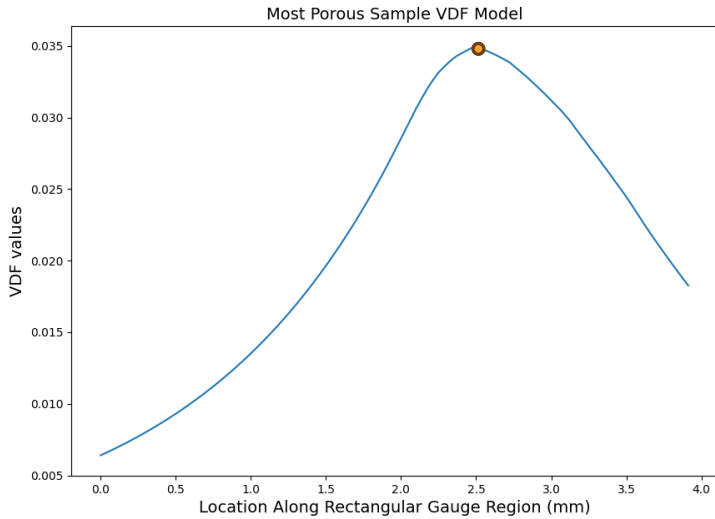
Obtain Geometries

Calculate Pore Metrics



- pores
 - axis_vectors
 - centroids
 - ellipsoid_surface_areas
 - ellipsoid_volumes
 - equivalent_sphere_diameters
 - nearest_neighbor_IDs
 - nearest_neighbor_distances
 - num_voxels
 - semi-axis_lengths

Results: Void Descriptor Function



| | Most Porous | Porous | Least Porous |
|---------------|-------------|---------|--------------|
| Max VDF value | 0.03496 | 0.00606 | 0.000175 |
| Location (mm) | 3.641 | 3.462 | 3.371 |

Results: Comparison – Fracture Locations



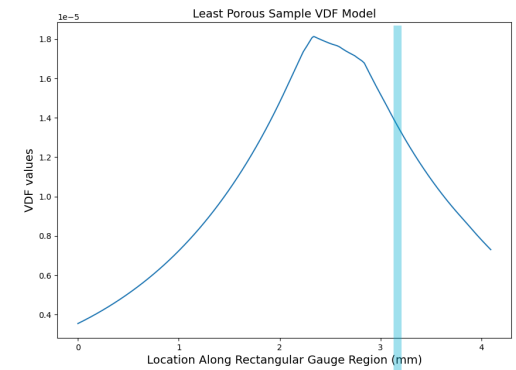
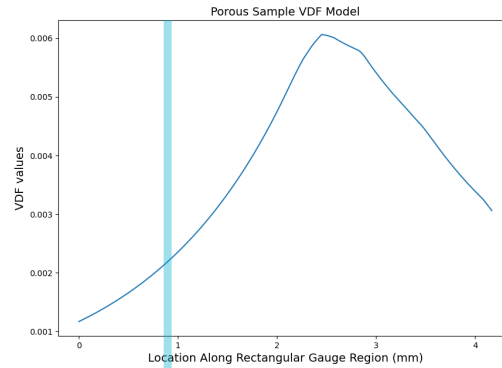
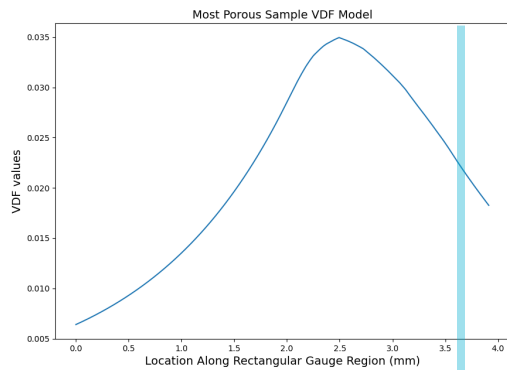
Least Porous

Porous

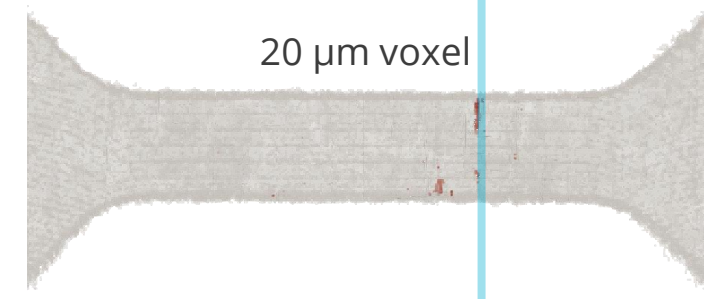
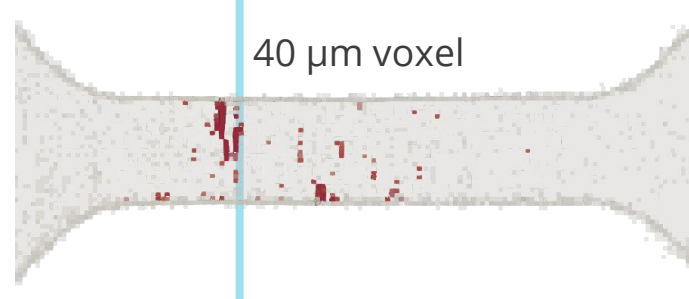
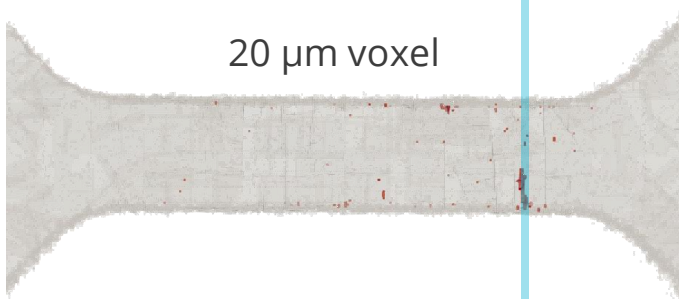
Most Porous

Scale is in mm

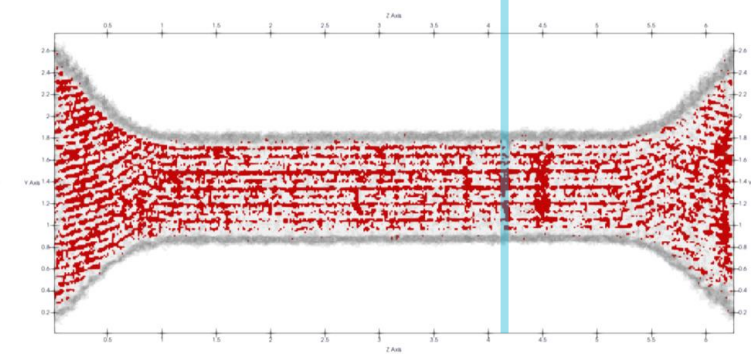
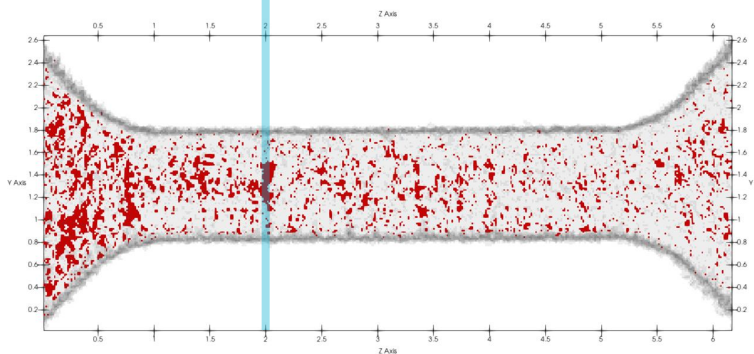
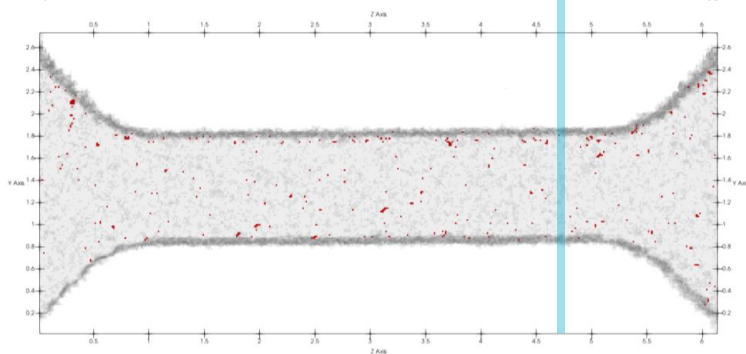
VDF



DNS



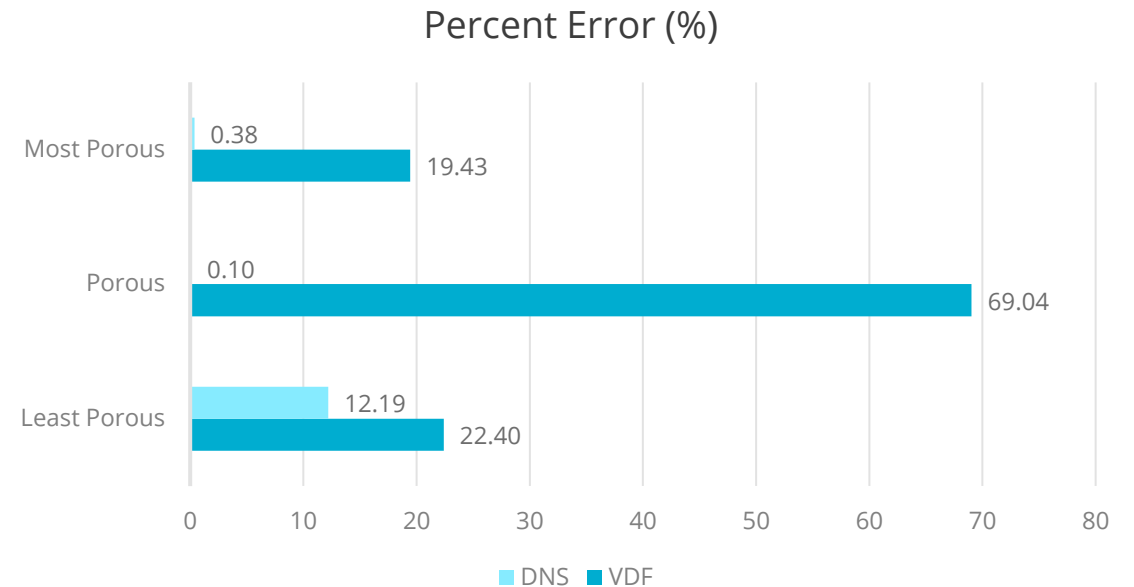
EXP





- VDF takes significantly less time than DNS (~0.269 seconds compared to ~25+ minutes)
- DNS showed a lower percentage error indicating a more accurate model
- Mesh resolution affects failure location accuracy.
- This project serves a stepping stone in advancing the broader scope of the research effort.

| | Fracture Location (mm) | | |
|-----|------------------------|--------|-------------|
| | Least Porous | Porous | Most Porous |
| EXP | 4.692 | 2.048 | 4.184 |
| DNS | 4.12 | 2.05 | 4.20 |
| VDF | 3.371 | 3.462 | 3.641 |



Acknowledgements



This research was conducted at the 2024 Nonlinear Mechanics and Dynamics Research Institute hosted by Sandia National Laboratories and the University of New Mexico.

Ivana would like to acknowledge the NNSA Minority Serving Institutions Internship Program (MSIIP) administered by ORISE on behalf of the NNSA for sponsoring her internship at NOMAD.

Sandia National Laboratories is a multimission laboratory managed and operated by National Technology and Engineering Solutions of Sandia, LLC, a wholly owned subsidiary of Honeywell International, Inc., for the U.S. Department of Energy's National Nuclear Security Administration under contract DE-NA-0003525.



1. Sames, W. J., List, F. A., Pannala, S., Dehoff, R. R., & Babu, S. S. (2016). The metallurgy and processing science of metal additive manufacturing. *International Materials Reviews*, 61(5), 315–360. <https://doi.org/10.1080/09506608.2015.1116649>
2. Lewandowski, J. J., & Seifi, M. (2016). Metal Additive Manufacturing: A Review of Mechanical Properties. In *Annual Review of Materials Research* (Vol. 46, Issue 1, pp. 151–186). Annual Reviews. <https://doi.org/10.1146/annurev-matsci-070115-032024>
3. Karlson, K. N., Skulborstad, A. J., Madison, J. M., Polonsky, A., & Jin, H. (2023). Toward accurate prediction of partial-penetration laser weld performance informed by three-dimensional characterization – Part II: μ CT based finite element simulations. *Tomography of Materials and Structures*, 2, 100007. <https://doi.org/10.1016/j.tmater.2023.100007>
4. Bergel, G., Karlson, K., & Stender, M. (2020). Assessing the Influence of Process Induced Voids and Residual Stresses on the Failure of Additively Manufactured 316L Stainless Steel. Office of Scientific and Technical Information (OSTI). <https://doi.org/10.2172/1593545>
5. Erickson, J. M., Rahman, A., & Spear, A. D. (2020). A void descriptor function to uniquely characterize pore networks and predict ductile-metal failure properties. In *International Journal of Fracture* (Vol. 225, Issue 1, pp. 47–67). Springer Science and Business Media LLC. <https://doi.org/10.1007/s10704-020-00463-1>
6. Watring, D. S., Benzing, J. T., Kafka, O. L., Liew, L.-A., Moser, N. H., Erickson, J., Hrabe, N., & Spear, A. D. (2022). Evaluation of a modified void descriptor function to uniquely characterize pore networks and predict fracture-related properties in additively manufactured metals. In *Acta Materialia* (Vol. 223, p. 117464). Elsevier BV. <https://doi.org/10.1016/j.actamat.2021.117464>
7. Thomas, M., Baxter, G. J., & Todd, I. (2016). Normalised model-based processing diagrams for additive layer manufacture of engineering alloys. In *Acta Materialia* (Vol. 108, pp. 26–35). Elsevier BV. <https://doi.org/10.1016/j.actamat.2016.02.025>
8. E. Voce. (1948). The Relationship Between Stress and Strain for Homogeneous Deformations, *J. of the Institute Metals*, 74:537-562
9. R. Hill. (1948). A theory of the yielding and plastic flow of anisotropic metals. *Proceedings of the Royal Society of London*, A193:281-297.



Experimental Data Analysis

- Automated fracture location
- Better inform data-driven predictive models
- Further analysis on Normalization energy values

Direct Numerical Simulation

- Full sample set simulations
- Smaller voxel size mesh simulations
- Fracture initiation (void)

Void Descriptor Function

- Optimization in progress
- Account for surface roughness